ANNUAL REVIEWS

Annual Review of Condensed Matter Physics

Spatial and Temporal Organization of Chromatin at Small and Large Scales

Helmut Schiessel

Cluster of Excellence Physics of Life, Technische Universität Dresden, Dresden, Germany; email: helmut.schiessel@tu-dresden.de

Annu. Rev. Condens. Matter Phys. 2023. 14:193–210

First published as a Review in Advance on November 9, 2022

The *Annual Review of Condensed Matter Physics* is online at conmatphys.annualreviews.org

https://doi.org/10.1146/annurev-conmatphys-040821-115729

Keywords

DNA, nucleosome, chromatin, loop extrusion, epigenetics

Abstract

DNA molecules with a total length of two meters contain the genetic information in every cell in our body. To control access to the genes, to organize its spatial structure in the nucleus, and to duplicate and faithfully separate the genetic material, the cell makes use of sophisticated physical mechanisms. Base pair sequences multiplex various layers of information, chromatin remodelers mobilize nucleosomes via twist defects, loop extruders create a system of nonconcatenated rings to spatially organize chromatin, and biomolecular condensates concentrate proteins and nucleic acids in specialized membraneless compartments. In this review, we discuss the current state of understanding of some of these mechanisms that influence the organization of the genetic material in space and time.

1. INTRODUCTION

DNA molecules of eukaryotic cells are complexed into a rather dense DNA-protein complex called chromatin. Because DNA carries genetic information, its packaging brings challenges and opportunities. How can the genetic information be accessed? Can DNA direct its own packaging? Is DNA packaged differently in different cell types? How can the cell disentangle identical copies of DNA molecules in preparation for cell division? How can the epigenetic information be passed on to the next cell generation? This review addresses these and other questions.

Knowledge in this field has exploded in the past 20 years. When I wrote my first review on the subject, entitled "The Physics of Chromatin," in 2003 (1), our understanding of this subject was rather patchy. Thanks to revolutionary experimental developments, large-scale computer simulations and sophisticated theories, knowledge has reached a level that I would not have expected in my lifetime. At the same time, there is a risk of getting lost in the abundance of information.

The format of this review is too brief to cover all the important developments in this field. Instead, I focus on some simple basic physical mechanisms and how they might be useful for cells. I do this for the small scales in Section 2 by discussing the nucleosome, the elementary packaging unit of chromatin, and for the chromosome at large scales in Section 3. The nucleosome, the most abundant DNA-protein complex (roughly three-quarters of the human genome are sequestered by nucleosomes), is a dynamic structure with a large number of surprising properties, and large-scale chromatin organization reveals a wide range of exotic new polymer physics, some of which are associated with very large timescales.

2. THE NUCLEOSOME

About three-quarters of our DNA is wrapped around protein cylinders, forming DNA-protein complexes called nucleosomes. This affects the accessibility of various proteins to the genetic material at both a local and a global scale. In this section, I focus on the local effects. Specifically, I discuss where nucleosomes prefer to sit along DNA molecules (nucleosome positioning, Section 2.1) and how dynamic processes give access to nucleosomal DNA (nucleosome breathing, Section 2.2; nucleosomes under force, Section 2.3; the role of twist defects for nucleosome repositioning, Section 2.4).

The core of the nucleosome consists of eight histone proteins, two copies of each type: H2A, H2B, H3, and H4 (2). These proteins interact with each other to form heterodimers, H2A-H2B and H3-H4. In the nucleosome, two H3-H4 dimers occur as a tetramer, interacting with each other through a four-helix bundle. The binding of two H2A-H2B dimers to the tetramer through a similar mechanism leads to the octamer around which 147 base pairs (bps) of DNA are wrapped. This results in a DNA-protein complex with a twofold symmetry in which the dyad passes through the central bp (**Figure 1*a***).

Histone-DNA interaction mainly involves the binding between negatively charged DNA phosphates and positively charged residues on the disk-like octamer. The sites are located at the 14 places where the minor groove of the DNA double helix faces the octamer. In terms of the superhelical coordinate (2), defined by the number of DNA helical turns with respect to the central bp, the binding sites occur at half-integer superhelical locations (SHLs) from -6.5 to $+6.5$. Each binding site mainly involves two DNA phosphates, one on each strand. Each dimer contributes three binding sites for the DNA molecules, leading to 12 binding sites organizing 121 bps. These binding sites fall into two categories: The four binding sites at ± 1.5 and ± 4.5, which involve two alpha helices at the histone dimer centers, are called $\alpha 1 \alpha 1$ binding sites, and the remaining sites (at SHLs ± 0.5, ± 2.5, ± 3.5, and ± 5.5) are called L1L2 binding sites and involve the binding to two adjacent loop structures at the ends of each histone dimer. The remaining two outermost

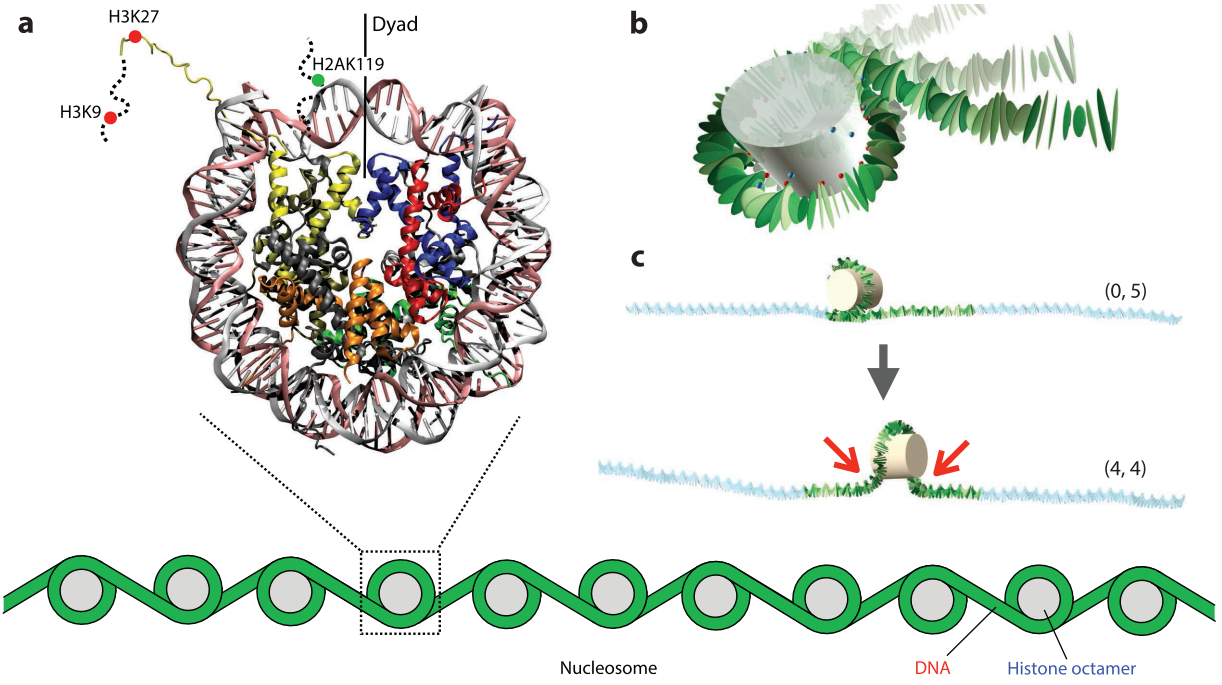

Figure 1

The nucleosome. (*a*) Crystal structure of the nucleosome core particle, which consists of the histone octamer and wrapped DNA. Together with the linker DNA, this forms the elementary repeat unit of chromosomes, the nucleosome. The histone proteins (shown in different colors) feature unstructured (and thus only partially crystallized) histone tails, two of which are sketched together with places of epigenetic tags, which are discussed in Section 3.3. Structure 1AOI (2) from the protein data bank. (*b*) A breathing nucleosome. (*c*) Nucleosomes under external forces are kinetically protected against transient tensions by high-energy transition states like (4, 4), where two DNA portions are strongly bent (*red arrows*). Experiments (3) show that the 601 nucleosome "rests" in the highly asymmetric metastable state (0, 5) before crossing this barrier. Panels *b* and *c* show a coarse-grained nucleosome model that was first introduced in Reference 4.

binding sites at SHL ±6.5 are formed by the binding of the H3 N-terminal extensions to the 13-terminal bps of the nucleosomal DNA termini. In general, the binding of the DNA to the central $(H3\text{-}H4)_2$ tetramer is stronger than to the H2A-H2B dimers (5). The resulting complex has a diameter of about 10 nm and is about 6 nm high.

The bending of the stiff DNA double helix is energetically costly. One can estimate the price using the wormlike chain (WLC) model (1), which treats the DNA as an elastic rod. Its bending stiffness follows from micromanipulation experiments (6). The following estimate for the bending energy (in units of the thermal energy k_BT) of nucleosomal DNA is not very precise as it assumes linear elasticity, homogeneous elastic properties of the DNA, and a constant curvature of bending:

$$\frac{E_{\text{elastic}}}{k_BT} = \frac{l_P L}{2R_0^2}. \qquad 1.$$

l_P is the DNA persistence length, about 50 nm, and L is the length of the bent part of the DNA. We only count 127 bps for L, as approximately 10 bps at each end are essentially straight. With 0.34 nm length per bp, $L = 127 \times 0.34\,\text{nm} = 43\,\text{nm}$. $R_0 \approx 4.3$ nm denotes the radius of curvature of the centerline of the wrapped DNA. This leads to $E_{\text{elastic}} \approx 58\,k_BT$. Note that the estimated bending energy is very high, many times the thermal energy. The total adsorption energy E_{ads}

gained by the wrapping of the DNA around the octamer must be even higher. An estimate of the difference between these two energies, the net adsorption energy E_{net}, follows from experiments discussed in Section 2.2. The actual values of $E_{elastic}$ and E_{ads} are not always relevant. For instance, nucleosome breathing discussed in Section 2.2 cares only about E_{net}. But in other cases, e.g., for nucleosome sliding (Section 2.4), the value of E_{ads} is relevant.

2.1. Nucleosome Positioning

The positions of nucleosomes along DNA are not random. On one hand, nucleosomes have to compete with other DNA binding proteins that bind to specific bp sequences. On the other hand, nucleosomes show sequence preferences themselves. The latter can be seen most clearly when mapping nucleosomes that have been reconstituted from their pure components, DNA, and histones, by salt dialysis (7). Nucleosomes show two types of positioning, rotational and translational (8). Rotational positioning describes the local positional preference of a nucleosome that, because of the helical nature of the DNA molecules, is an orientational preference. Nucleosomal DNA prefers GC (guanine–cytosine) bp steps, where the DNA major groove faces the octamer, and AA (adenine–adenine), TT (thymine–thymine), and TA (thymine–adenine) steps, where the minor groove faces the octamer (7, 9, 10). Even random bp sequences typically show preferred rotational locations in about every 10-bp stretch, the DNA helical repeat (11). However, this does not exclude the possibility that bp sequences have evolved to position nucleosomes in specific orientations. Translational positioning refers to preferences of nucleosomes to occupy or avoid larger stretches of DNA. Nucleosomes are attracted to DNA regions rich in GC content, i.e., sequences that contain a large fraction of guanine (G) and cytosine (C; 12–16). This can be best detected when looking at genome-wide averages of genomic landmarks, e.g., transcription start sites (see below).

What are the physical origins of rotational and translational nucleosome positioning? This can be best tested by using coarse-grained DNA models with sequence-dependent mechanical and geometrical properties, as, e.g., the rigid bp model (17) or the 3SPN (3 sites per nucleotide) model (18). For instance, in the rigid bp model the bps are treated as rigid bodies, the spatial position and orientation of which are described by six degrees of freedom per bp step. It assumes nearest-neighbor interactions with a quadratic deformation energy between successive bps. Importantly, each type of bp step has its own elasticity and intrinsic shape derived from DNA-protein cocrystals (17) or from all-atom molecular dynamics simulations of DNA oligomers (19). Such models show that the periodic bp step preferences reflect the preference of nucleosomes for intrinsically curved DNA, causing rotational positioning (4, 20–22). It can be confusing at first that some of the bp steps, especially TA and GC steps, have intrinsic geometries that are not consistent with the rotational positioning requirements and, in fact, even oppose them. This reflects the fact that bp steps are part of a longer bp sequence and that only longer sections of a sequence, such as, e.g., TTAA, show the proper intrinsic bendedness. Remarkably, this is even predicted by the rigid bp model, a purely local model, in which the physical properties of each bp step depend only on the bp step itself but not on the larger sequence in which it is embedded (22).

Even more complex is the physics underlying translational positioning. Because the elastic energy to bend DNA into a nucleosome is very high, one might expect that the translational preferences for GC mean that GC-rich DNA is softer on average than TA-rich DNA. However, a careful study of nucleosome models based on the rigid bp model showed that it is not energy but entropy that dominates the GC dependence of the free energy of nucleosomal DNA (23). This in turn means that softer (i.e., GC-rich) DNA stretches prefer to be nucleosome free to increase the entropy of the whole system. A possible way to solve this conundrum is to use a multiharmonic model (23) that uses different parameterizations for free and wrapped DNA, namely based on

computer simulations of oligonucleotides (19) and on cocrystals of DNA-protein complexes (17). This in turn leads to a model that qualitatively shows the right GC preferences of nucleosomes. However, the problem goes deeper. Saturation in the GC content of nucleosomes reconstituted on the genome of baker's yeast (7) indicates that such a system is never equilibrated (23). In fact, the density of nucleosomes is practically constant for stretches of 2,000 bps, suggesting that reconstituted chromatin only equilibrates locally but does not achieve global equilibration. Taking this into account, the multiharmonic model also shows good quantitative agreement between model and experiment (23).

To which extent are nucleosomes positioned by bp sequences in vivo? There are various experimental methods to map nucleosomes in vivo, including the digestion with micrococcal nuclease (10), ATAC-Seq (24), chemical cleavage-based techniques (25), and nucleosome footprinting techniques (26). The degree and type of positioning might depend on the organism. For instance, unicellular organisms tend to have a dip in GC-content around transcription start sites. It has been speculated that the resulting nucleosome depletion "may facilitate transcription initiation and assist in directing transcription factors to their appropriate sites in the genome" (7, p. 365). These nucleosome depleted regions in turn act as fixed boundaries from which nucleosomes form a more or less periodic array as the result of statistical ordering (27). Remarkably, as the transcription termination sites also constitute a nucleosome depleted boundary, nucleosomes on genes form relatively regular nucleosome "crystals," as demonstrated by the ordering of genes by length (28). Nucleosomes reconstituted on the yeast genome do not show statistical order, because the nucleosome line density is much lower in this case (7).

Although the organization of nucleosomes in yeast and other unicellular organisms seems to be dominated by antipositioning and statistical ordering, the organization of multicellular organisms appears to follow other principles. Looking at genome-wide averages of the GC content around transcription start sites, one finds broad peaks that increase with the complexity of the organism (16). These peaks might have various functions, including functions involving nucleosomes. As this feature is found in multicellular life forms, the hypothesis imposes itself that these nucleosome-attracting regions "restrict access to regulatory information that will ultimately be utilized in only a subset of differentiated cells" (29, p. 1). However, this idea is countered by results that find stronger intrinsic nucleosome-attracting regions for housekeeping genes than for tissue-specific genes (30). Even worse, the nucleosome density at transcription start sites in housekeeping genes is depleted in somatic cells. A possible explanation is that these GC peaks are meant for sperm cells (30). During spermatogenesis most of the bulky histones are replaced by protamines, which allow the creation of small and highly mobile sperm cells in large numbers. This, however, means loosing epigenetic information written in posttranslational modifications of the histone tails (**Figure 1*a***). Interestingly, however, some of the nucleosomes are retained (e.g., 4% in humans; 31). The retention sites correspond to the peaks in GC content around transcription start sites where the most stable nucleosomes are located (16, 30). This might allow epigenetic information to be transmitted from the father to the offspring. Remarkably, the high GC peaks are not only found at housekeeping genes but also at genes that regulate development. However, also in human somatic cells, many nucleosomes are positioned by mechanical signals from the underlying bp sequence such as the positioning of six million nucleosomes around nucleosome-inhibiting barriers (15).

The fact that many nucleosomes are positioned on DNA and change their positions rather slowly raises the question of access to DNA. In the next section, I discuss the intriguing possibility that nucleosomes might be essentially "transparent" to other DNA binding proteins because of their intrinsic dynamics.

2.2. Nucleosome Breathing

Sections of nucleosomal DNA temporarily unwrap from the protein cylinder simply because of thermal fluctuations (see **Figure 1*b***). This process, called nucleosome breathing or site exposure, can give other proteins a window of opportunity to bind to nucleosomal DNA (32, 33). Nucleosome breathing had already been observed in 1995 by measuring the accessibility of restriction sites inside nucleosomal DNA to the corresponding enzymes (34, 35) and later by Förster resonance energy transfer (FRET) experiments (36–42) and atomic force microscopy (43, 44). These experiments demonstrated that nucleosomes temporarily expose their DNA, including even the stretch at the middle of the wrapped portion. The probability for a nucleosomal DNA site to be accessible decays roughly exponentially toward the dyad (45). Importantly, such experiments revealed that nucleosomes can be very different from each other as a result of the sequence-dependent mechanical properties of their wrapped DNA (35, 38, 46–49; cf. Reference 32 for a review). The nucleosome bound to the positioning sequence Widom 601, a sequence selected out of a large pool of random DNA owing to its high affinity to the histone octamer (50), was found to show highly asymmetric breathing behavior with one half being much more accessible than the other half (35).

New insights were gained by a new type of experiment in which an ensemble of breathing 601 nucleosomes was observed through X-ray diffraction (51). Through contrast matching between the solvent and the protein core, only the DNA could be "seen." The unwrapping states of the nucleosomes were determined through an ensemble optimization method in which the contributions from different conformations (including the fluctuations of the unwrapped DNA) were accounted for, allowing even to distinguish between the two ends of the unwrapped DNA. The data clearly showed that the 601 nucleosome breathes in a highly asymmetric fashion, consistent with the earlier result (35). Notable is the change seen in breathing behavior when the ionic strength is increased and, therefore, the adsorption energy decreased. The change is not smooth, but the nucleosomes jump from being fully wrapped to a state in which about the five leftmost binding sites have opened. This "spring-loaded latch mechanism" (51, p. 779) was speculated to be caused by an outer soft DNA stretch followed by a stiffer inner stretch. Once the adsorption energy is small enough that the outer stretch opens, the inner stretch cannot withstand the mechanical tension of its stiffer DNA and opens up in a jump-like fashion.

A computational study of the coarse-grained 601 nucleosome (see **Figure 1*b***) corroborated this interpretation (52) and also allowed extraction of the adsorption energy of the DNA to the octamer as a function of the salt concentration. It also demonstrated the extreme sensitivity of nucleosome breathing to the involved sequence. A replacement of just two bp steps by TA-steps in the stiff section destroys the spring-loaded latch mechanism. This might have biological implications. In Reference 53, the idea was put forward that there could be a cooperativity between two proteins, A and B, which have their two binding sites within a nucleosome. If the binding site of A is more outward in the nucleosome than the binding site of B, then after binding of A, the target site of B becomes more easily accessible. For a spring-loaded nucleosome like 601, this effect can be amplified greatly, but changes of a few bp steps would eliminate this effect. This strong sensitivity of nucleosome breathing also affects the measurements with restriction enzymes mentioned above, as this method requires modifying the bp sequence to incorporate restriction sites. For instance, in Reference 35, 15 bps of the 601 sequence were changed to create 12 restriction sites across almost the entire wrapped DNA portion. In a simulation study (54), these modifications dramatically changed the accessibility of most interior sites by an order of magnitude.

The simulation model (52) that is based on the nucleosome crystal structure and uses the rigid bp model for DNA leads to sequence-dependent elastic energies that, remarkably, are in a similar

range to what is extracted from the simple WLC model (Equation 1; which does not include the sequence dependence). For instance, in the simulation the elastic energy of the 601 nucleosome is found to be about 68 k_BT, which is close to the 58 k_BT of the WLC estimate. Under physiological conditions the adsorption energy is estimated to be on the order of 80 k_BT, showing that the two energies nearly cancel. This means that the DNA is rather weakly adsorbed on the octamer with a binding energy of about 1 k_BT for each of the 14 binding sites. Similar numbers follow from a fit of the simpler model to older data extracted with restriction enzymes (45).

The discussion so far might give the impression that all the nucleosomal DNA is readily accessible to DNA binding proteins, even stretches deep inside well-positioned nucleosomes. However, even though all sites inside a nucleosome are in principle accessible, the fraction of time a site is encountered as open decays roughly exponentially toward the center of the wrapped DNA. This leads to the question of timescales. Kinetic measurement based on FRET revealed that the outer DNA of the 601 nucleosome (bp 17 and 18 counted from the terminus of the wrapped portion) has a characteristic waiting time for unwrapping of only 0.25 s, but times then increase dramatically to 1 min 10 bps further in and even to 10 min for another 10 bps further in (41). This strong increase in the waiting time might reflect the fact that the DNA is not homogeneously bound but that there are stretches of stronger interaction, one starting about 20 bps inside, as shown experimentally (5). Atomistic molecular dynamics simulations (55, 56) can help to understand better the details of the unwrapping process, e.g., the role of an "H3-latch" and of the histone tails (56).

The fact that unwrapping rates for inner portions are excessively low means that nucleosomes are not completely "transparent" to other DNA binding proteins. The authors of Reference 41 concluded that these low unwrapping rates together with a variability of nucleosome positioning could explain dispersion in response times of cells. We next discuss how nucleosomes react to external mechanical tension.

2.3. Nucleosomes Under Force

Nucleosome breathing experiments allow estimation of the net adsorption energies gained by DNA adsorption on the histone octamer to be about one k_BT per binding site, with a total of 14 binding sites. From this, together with the wrapping length of about 50 nm, one would expect that a moderate force of about 1 pN would be enough to unravel a nucleosome. This contrasts the much larger forces observed in micromanipulation experiments (57). When an array of 17 nucleosomes was pulled apart by an optical trap with a constant rate, characteristic drops in tension occurred, reflecting the unwrapping of the DNA from individual nucleosomes. Remarkably, this happened at forces around 20 pN, about 20 times greater than expected based on breathing experiments. The typical force depended roughly logarithmically on the pulling rate, pointing toward the existence of an energetic barrier that was estimated to be 35 k_BT high.

However, it was subsequently pointed out that the barrier might be caused by the geometry of the nucleosome [see Reference 58 and subsequent work (59–68)]. The nucleosome under force f needs to rotate by 180 deg during the unwrapping of the last DNA turn. This leads to a transition state, the half-turned nucleosome, where each DNA arm needs to make a 90 deg bend as it enters the wrapped portion of the nucleosome (see state (4, 4) in **Figure 1*c***). Interestingly, the act of pulling on the nucleosome is the cause of the energy barrier with a height that scales as $\sqrt{f}$. The experiment did not provide direct insight into the interactions between the DNA and the histone octamer, but it taught something crucial: Nucleosomes are protected against transient tension by the buildup of a kinetic barrier (58). This is important in the cell with its large number of motor proteins pulling on the DNA.

More details about the unwrapping path of a nucleosome under force was provided by an experiment (3) in which FRET and micromanipulation were combined. For the 601 nucleosome it

was found that it always unwraps from one end first and that it is always the same end. As predicted by the model mentioned above (58), the nucleosome under force gets stuck in a metastable state with one turn of DNA remaining wrapped, leading to straight DNA arms [see, for example, state (0, 5) in **Figure 1*c***]. This single turn prefers to include one of the two straight end sections. Because the sequences used in the experiment were nonpalindromic, the bending energies in these two configurations differ substantially. A nucleosome model (69) using the rigid bp model (**Figure 1*c***) leads to predictions consistent with the findings of the experiment (3). It also explains the surprising finding (3) that for a bp sequence in which the inner two quarters are flipped, the nucleosome always unwraps from the other end.

A long series of experiments, computer simulations, and theory helped to reveal the richness of the physical properties of the nucleosome: The spool geometry together with the DNA stiffness causes a transient barrier under force, and the nonuniform features of both the wrapping path and the intrinsic DNA shape modulate the path over that barrier. Using this knowledge, one can computationally design bp sequences that lead to very stable nucleosomes with an Achilles' heel: As soon as an external force is applied, they easily fall apart (70). Such nucleosomes might have evolved at places on the genome where it is beneficial to undermine the kinetic force protection. For example, as the two chromosomes get pulled apart during anaphase, ultrafine bridges form between fragile sites along the genome (71, 72), causing a signal for a repair mechanism, triggered by the appearance of bare DNA (73). In such a context, fragile nucleosomes could act as force sensors promoting the repair.

The forced nucleosome unwrapping experiment (57) was originally performed to learn about the interactions between the DNA and the histone octamer, but these interactions were masked by the occurrence of a kinetic barrier caused by DNA bending. In the meantime, the same experimental group managed to circumvent this problem. The idea is to unzip DNA, i.e., pulling its two strands apart, using a micromanipulation setup. If a nucleosome is present on the DNA molecule, once the unzipping fork reaches the nucleosome, the unzipping slows down (5). By pulling with a constant force of 28 pN and observing pausing patterns during unzipping, it was found that each of the 14 binding sites is actually composed of two interaction points, one on each DNA strand. In addition, the data revealed that the binding strength is not constant along the nucleosomal DNA but shows three broader regions with stronger interactions, with the strongest region around the dyad.

2.4. Twist Defects on Nucleosomes

Nucleosomes can also change their positions along DNA. This is mainly caused by twist defects in the wrapped DNA that occur spontaneously owing to thermal fluctuations or can be injected by dedicated motor proteins. We first discuss spontaneous repositioning. This phenomenon, called nucleosome sliding, allows for equilibration of nucleosomes along DNA. The spontaneous repositioning of nucleosomes is a rather slow process (74), which suggests that nucleosomes can only equilibrate locally, and this is consistent with my discussions in Section 2.1. Two mechanisms have been proposed, both based on thermally induced defects within the nucleosomal DNA: single bp twist defects (a missing or an extra bp) (75–77) and 10-bp loop defects (78, 79). New simulation studies (80, 81) suggest that twist defects are the dominant mode of repositioning but also loops might be at play for certain bp sequences. The underlying computational models use the coarse-grained 3SPN DNA model, which is attracted electrostatically to the oppositely charged protein cylinder modeled by a coarse-grained protein model called atomic-interaction-based coarse-grained (AICG). Remarkably, as a result of this interaction, a proper nucleosome forms. Over the course of time, the position of the octamer along the DNA molecule changes via

1-bp steps caused by twist defects. In addition, strongly positioned nucleosomes also occasionally "tunnel" through the high barriers in the energy landscape via loop defects.

Also a recent experimental observation suggests that both types of defects might underlie nucleosome sliding (82). The experiment uses a micromanipulation setup in which a nucleosome-containing DNA molecule is unzipped, similar to the experiment mentioned above (5). The application of a slightly lower force (23 pN instead of 28 pN) ensures that the unzipping fork stops at the nucleosome. By repeatedly pulling and relaxing the two DNA strands, the position of the nucleosome was determined with a 2-bp resolution at each probing cycle. Remarkably, nucleosomes containing a histone H2A variant, called H2A.Z, showed two types of movements: frequent small-scale movements, probably caused by twist defects, and longer-ranged repositioning events on the timescale of minutes, possibly caused by loop defects.

In vivo there are chromatin remodelers at work that use ATP to move nucleosomes along DNA. Experiments based on cryo-electronmicroscopy (83–85) and simulations (86) suggest that at least some of them induce twist defects in the nucleosomes. Whereas the older picture of twist defects is that they enter from the end of the wrapped portion, the remodelers seem to inject a twist-antitwist pair inside the nucleosomal DNA. Chromatin remodelers might help nucleosomes to equilibrate their locations along DNA (87), but they might also perturb the intrinsically preferred positioning of nucleosomes, together with other proteins that compete for DNA target sites (14). The efficiency of a remodeler might depend on the local elasticity of the DNA stretch that needs to be deformed (86). A new experiment (88) demonstrated that already upon binding of the remodeling complex, the bound DNA deforms into an A-DNA-like conformation. This suggests that even before the ATP-consuming step, the DNA is primed for the actual twist defects production. Finally, for remodelers to decide to act on the right nucleosome at a given time, a kinetic proofreading mechanism has been put forward (89, 90).

3. CHROMATIN AT LARGE SCALES

In this section, I discuss chromatin at much larger length scales. I skip intermediate length scales, such as the structure directly above the nucleosome, where the view has shifted away from regular fiber-like structures to that of a rather uniform melt of nucleosomes (91, 92) or of heterogeneous groups of nucleosomes, so-called clutches (93, 94). In general, a lack of quantitative experiments at the mesoscale currently makes it difficult to discriminate between different models. The situation was similar for large-scale chromatin a few years ago but has improved dramatically since then. An understanding of mesoscale chromatin organization is expected to improve our understanding of how nucleosomes are involved in larger-scale organization and, in particular, help us gain a better understanding of the concrete structures that underlie large-scale organization.

Remarkably, even without a good understanding of mesoscale organization, one can get a long way by starting from the fact that DNA molecules are long polymers and asking about the polymeric state of DNA molecules in the nucleus (95). Until 10 years ago, most scientists assumed that DNA molecules are in one of the standard polymeric states. However, new experimental methods suggested in 2009 that DNA molecules have an exotic state called the fractal globule, discussed in Section 3.1. This is followed by Section 3.2, which gives a deeper insight into why such states occur. An analogy to nonconcatenated polymer rings or loops proves essential. Surprisingly, true nonconcatenated loops really exist as a central motif to organize chromatin on larger length scales, because cells use dedicated motors called loop extruders to produce them. **Figure 2** gives an overview of the progress in our understanding. In Section 3.3, the nucleosome surprisingly comes back into focus as the main organizer of chromosome structures on very large scales.

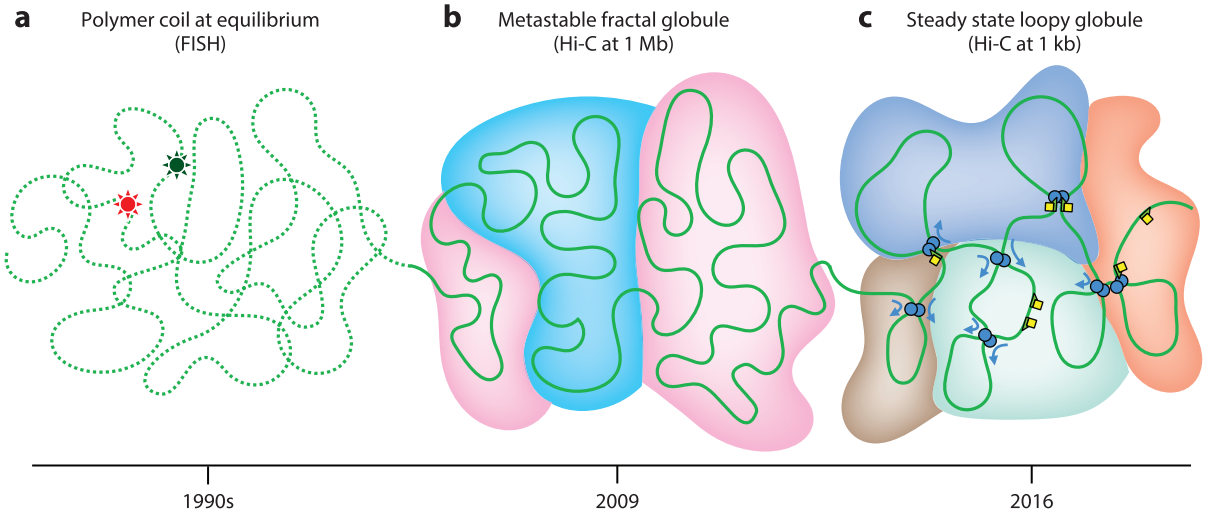

Figure 2

Paradigm shifts in large-scale chromatin organization. (*a*) FISH experiments on chromosomes in the 1990s suggested that DNA conformations in interphase chromosomes (interphase is the resting phase between successive mitotic divisions of a cell) behave like random polymer coils at equilibrium. (*b*) Chromosome conformation capture, specifically Hi-C data at 1 Mb resolution, suggested in 2009 that the chromosomes are in a metastable polymer state, the fractal or crumbled globule. In addition, it mapped two subcompartments (indicated here by colors). (*c*) More recently, Hi-C experiments at 1 kb resolution point toward a loopy globule state, a steady state maintained by the continuous action of molecular motors, called loop extrusion complexes. In addition, new subcompartments have been identified. Abbreviation: FISH, fluorescence in situ hybridization.

3.1. From Classical Polymers to Fractal Globules

The size of an isolated polymer scales with the number N of monomers as

$$R \propto N^{\nu}, \qquad 2.$$

with $\nu = 1/2$ in the absence of excluded volume (random walk, ideal chain) and $\nu \approx 3/5$ when there is excluded volume between the monomers (self-avoiding walk, swollen coil) (96). The ideal case $\nu = 1/2$ can be achieved by tuning the second virial coefficient between monomers to zero or—what is important here—when one has a semidilute or dense solution of polymers. Polymers then show overlapping ideal chain configurations because monomers from other chains screen the excluded volume (96). The classical polymer physics view has been tested by FISH (fluorescence in situ hybridization) experiments in which pairs of loci on the DNA are marked and their distance is measured (97; **Figure 2*a***). However, the classical view of overlapping polymers is challenged by chromosome painting experiments that show that chromosomes do not mix but instead each lives in their own territory (98). Neglecting this inconsistency, one can model chromosomes as polymers inside boxes of the size of their territories, which gives a satisfactory fit (99) to the data (100). Notably, recent experiments and computer simulations suggest that chromosomes may correspond to polymers under poor solvent conditions (101–106). In the classical case, this would still lead to $\nu = 1/2$ (107), but unlike for a good solvent polymer in a box, for nuclei with a volume larger than the total volume of chromosomes, chromosome-free regions appear (104).

Experiments based on Hi-C, a chromatin conformation capture technique, showed, however, that chromosomes do not behave as classical polymers (108). In Hi-C, chromosomes are crosslinked and the connected DNA pieces are sequenced, allowing construction of contact maps of chromosomes. Averaged over all pairs of contacts, Hi-C found that the contact probability

p_c decays inversely proportional to the number g of bps in between two contact points, $p_c \propto g^{-1}$ (108), in contrast to $p_c \propto g^{-3/2}$ for ideal chains. This, according to the authors (108), might be explained by an idea going back to 1993 (109), where Grosberg et al. speculated that chromosomes could not show equilibrium polymer configurations as these would be too much entangled for their processing in the nucleus. Instead, similarities with collapsed globules were expected. Such a globule forms when a swollen polymer in a good solvent is suddenly exposed to poor solvent conditions. This leads to a hierarchical collapse into droplets of droplets, etc. As the original swollen coil was hardly entangled, so too was the collapsed globule. However, the hierarchical conformation suggests rather that $p_c \propto g^{-4/3}$. For deterministic space-filling fractal curves, one can construct values ranging from $-4/3$ down to -1 by increasing the degree of interdigitation between the involved subunits to an extreme (110). In computer simulations of collapsed globules in Reference 108, the -1 slope could only be reached by a rather unphysical collapse but not under less extreme conditions (111).

The question remained what a polymer collapse has to do with real chromosomes and why the structures should be interdigitated. The problem of these nonequilibrium structures is that they depend on the initial conditions of the system and that the chosen initial conditions did not correspond to the biological system. The way to arrive at a consistent view required the consideration of timescales.

3.2. From Polymer Rings to Loop Extrusion

Based on Reference 112, the equilibration times of human chromosomes was estimated to be about 500 years (113). Large relaxation times for long polymers in dense solutions are caused by their confinement in tube-like cages formed by other chains, out of which they can only escape through reptation, a slow snake-like motion (96). In addition, chromosomes start out in mitosis as compact structures in which they are not entangled with each other. As the chromosomes expand—leaving the mitotic stage—they collide with each other. Given the huge reptation timescales, they stay unentangled, each within their territory, and do not mix within a cell cycle. Thus, one might forget about the chain ends altogether and close each chain into a ring (113). Because of the initial compact nonconcatenated mitotic state, these chromosome rings are also not concatenated. This theoretical line of arguments (114) suggests that one can understand the metastable conformations of real chromosomes by studying the equilibrium structure of a solution of nonconcatenated rings (see **Figure 3**).

What do semidilute solutions of nonconcatenated rings look like? Large-scale computer simulations of solutions of nonconcatenated polymer rings show features that are substantially different from solutions of linear polymers (115). Notably, rings under these conditions avoid overlapping, show a compact structure with an overall size that scales like $N^{1/3}$, and are self-similar on all length scales (i.e., stretches of g monomers have sizes that scale like $g^{1/3}$), and the contact probability between monomers decreases with genomic distance as $1/g^{1.1}$ (115, 116), which is compatible with Hi-C data (108).

Surprisingly, nonconcatenated rings are not just a theoretical construct to explain chromosomal territories. Instead, cells actively produce nonconcatenated loops in at least two contexts, as became clear when contact maps produced by Hi-C measurements reached higher resolutions. **Figure 4*a***, **subpanel *i***, depicts schematically a low-resolution contact map of a chromosome [at megabase resolution (1 Mb); 108] and **Figure 4*a***, **subpanel *ii***, shows a high-resolution zoom onto the diagonal at the right [at kilobase resolution (1 kb); 117]. The low-resolution version shows a checkerboard pattern with the red tiles having a high density of contacts and the blue tiles a low density of contacts. There are two compartments, A and B, corresponding to euchromatin and

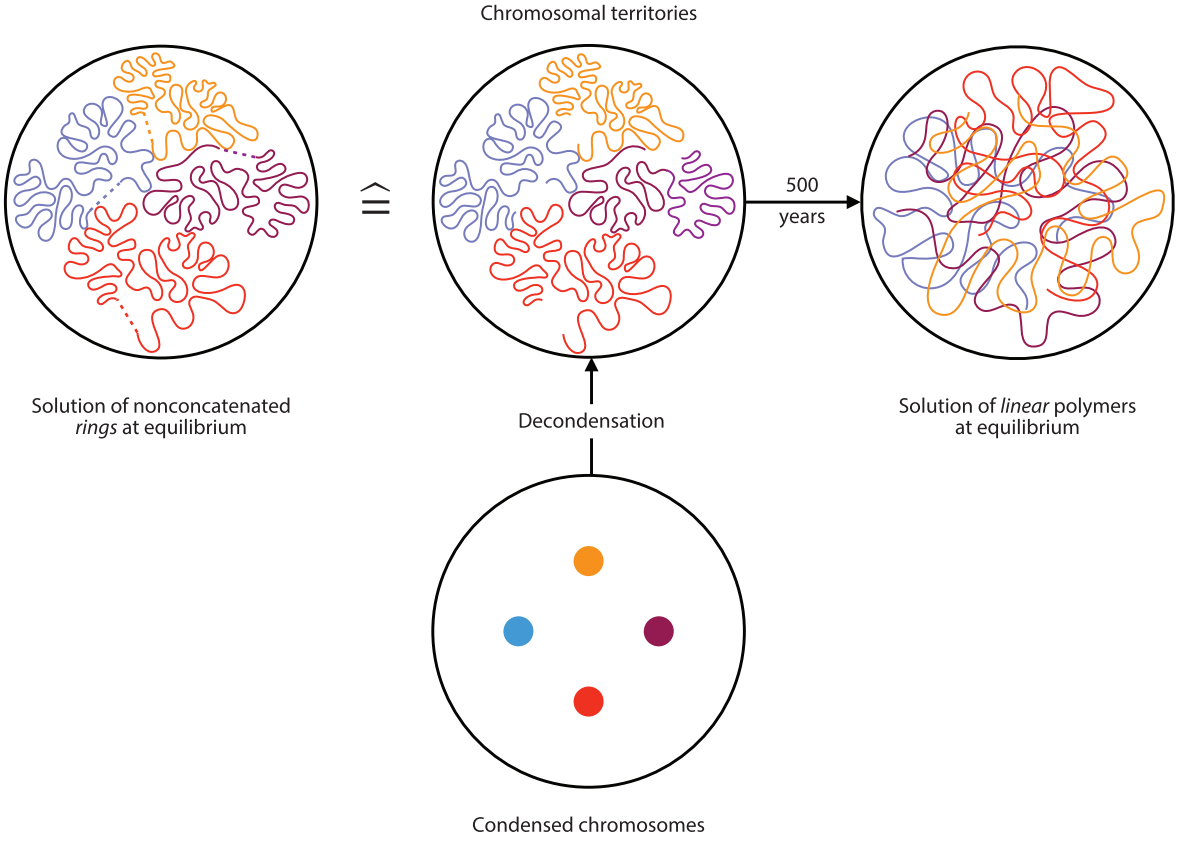

Figure 3

Large-scale organization of chromosomes. (*Top middle*) Chromosomal territories in interphase. These follow from the decondensation of the compact chromosomes (*bottom*) after cell division. The organization of chromosomes in interphase is an extremely long-lived metastable state. Human chromosomes need 500 years to mix (*top right*). The metastable demixed state is related to the equilibrium state of a solution of nonconcatenated ring polymers (*top left*), constructed theoretically through ring closure (*dashed lines*).

heterochromatin, respectively, each producing half of the high-density tiles. We discuss this further in the next section.

The checkerboard pattern at low resolution was expected. By contrast, the findings at higher resolution revealed unexpected mysterious structures, called topologically associated domains (TADs) or contact domains (117). These are tiles of even higher contact density along the diagonal (see **Figure 4*a***, **subpanel *ii***), and have a 185 kB median length in human. Surprisingly, each of the thousands of domains only has higher contact within itself, but not with other TADs. What could isolate them from each other? Furthermore, the borders of TADs are typically written into the bp sequence, with each motif being about a dozen bps long. They are called CTCF motifs because they serve as binding sites for the insulator protein CTCF. Rao et al. (117) made the strange observation that these sequences act as borders of TADs only if they are in a convergent orientation (the motif is nonpalindromic, so it can be assigned a direction along the genome). Something causes the DNA to form a loop, bringing these two CTCF motifs into spatial contact, but only if they happen to point in the "right" orientation along the genome. How could the two CTCF motifs know about their relative orientation as they are typically about 200 kB apart from each other?

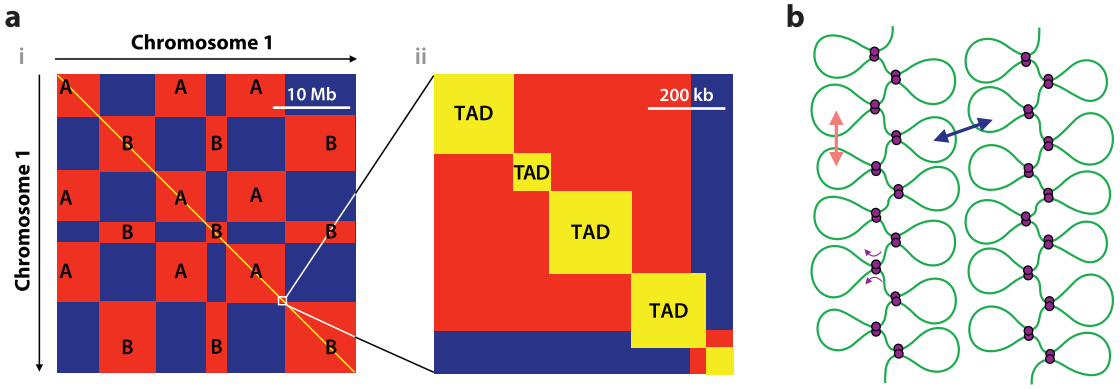

Figure 4

(*a*) Schematic view of a contact map of a chromosome at two different resolutions. (*i*) Low-resolution contact map with euchromatin (indicated by A) and heterochromatin (indicated by B). (*ii*) A high-resolution zoom onto the diagonal of subpanel *i* reveals TADs (see text for details). (*b*) Sketch of the loop structure of a mitotic chromosome produced by condensin (*double disks*). Loop repulsion within and between chromatids is indicated by double arrows. Abbreviation: TAD, topologically associated domain.

As discussed above, the chromosomes' topology has effectively an isolating effect, causing chromosomal territories. This requires the large timescales involved for the dynamics of whole chromosomes. TADs are much shorter and would mix quickly. If TADs were true nonconcatenated loops and not just a theoretical construct, they would all be isolated from each other. This turns out to be true. The cell constantly uses energy to maintain the existence of nonconcatenated loops by using special motor proteins, called cohesins. Cohesins act as so-called loop extruders (118). Extrusion complexes contain two DNA binding subunits tethered together. Initially, these two subunits bind nearby on the DNA. They then move in opposite directions along the DNA while bridging these increasingly distant chromosomal sites, thereby extruding a DNA loop. The spooling of DNA into the loop continues until the subunits encounter CTCF proteins bound to flanking, convergently arranged CTCF binding sites that block further extrusion (see **Figure 2*c***). As a result, TADs are dynamical systems of loops that are nonconcatenated with each other. Because nonconcatenated polymer loops do not mix, TADs are spatially separated from one another. This can be seen in detailed computer simulations (119–121). Through genome editing one can even flip, add, or remove CTCF motifs and show through contact maps that the TADs change as expected (122).

Although the biological role of TADs is still fairly unclear, the reason behind the second known example of loop extrusion is understood. These loops are needed to separate identical DNA molecules after duplication, leading to the iconic X-shaped mitotic chromosome. The free energy cost for overlap of two polymer coils despite excluded volume is only about one k_BT (123). This means that cells need to expend energy to separate the two DNA molecules. However, how can the two identical DNA molecules be distinguished from one another and be pulled apart? The repulsion of nonconcatenated loops is used here, produced by another loop extruder, called condensin (124–126). When condensin molecules start to act on the DNA molecules, they create loops, shortening each chromosome lengthwise. As the loops are nonconcatenated, they repel each other (see **Figure 4*b***). On one hand, this creates the desired repulsion between the chromosome pairs that are kept together only at their centers, the centrosomes. On the other hand, the loops along each chromosome stiffen the complex. The result of this process is the mitotic X-shaped chromosome, as demonstrated in a computer simulation (127; see also 120, 121). As the two DNA copies still suffer from entanglements when they are driven apart from each other, a specialized

protein, topoisomerase II, resolves these entanglements by letting the DNA double helices pass through each other. Mitotic chromosomes can be reconstituted even without nucleosomes (128), but if topoisomerase II is absent, a different structure, called sparkler, forms as a result of loop extrusion (129, 130).

3.3. Epigenetic Inheritance

A problem that cells encounter is how information about the cell type can be passed on to the two daughter cells. As all cells carry the same genetic information, it is obvious that different cell types express different genes, and this extra amount of information needs to be "inherited" by the daughter cells. This belongs to the realm of epigenetics, which is defined as processes that influence the function and expression of genes and that are long-lived, such that they are transmitted through mitosis (131). To explain how such information can persist through cell divisions, we need to look at the molecular mechanisms of epigenetics. There are two main mechanisms (131): Besides DNA methylation (not discussed here), there are posttranslational modifications (methylations, acetylations, etc.) of the histone proteins. In this case, specific amino acids, typically in the tails, carry specific tags (**Figure 1*a***). How these epigenetic tags are transmitted through mitosis is not yet understood.

In preparation for cell division, the genetic material needs to be duplicated. It is known experimentally (132) that during this process the nucleosomes are randomly distributed between the two newly formed DNA double helices. The resulting empty stretches are then filled with new nucleosomes made from new histones. As a result, only half of the nucleosomes still carry epigenetic marks. How do the daughter cells bring the marks back onto the new nucleosomes? This is crucial in order to maintain cell identity over many cell generations.

I focus on the epigenetic tag H3K9me3 on histone H3 (131; **Figure 1*a***). Nucleosomes with this tag belong to heterochromatin, the part of chromatin that is more densely packed and less accessible, as opposed to euchromatin. The checkerboard pattern of hetero- and euchromatin in contact maps (**Figure 4*a***) is closely mirrored by the H3K9me3 tags (117). These tags come in long blocks of nucleosomes (median length ≈50 nucleosomes in humans; 133), interrupted by blocks of nucleosomes without this tag. Explanations of how the missing tags come back onto the nucleosomes usually involve 1D models (133, 134) in which the repressive tags spread along the string of nucleosomes and stop at postulated insulators (133, 134). However, this 1D picture seems unlikely to do justice to the real 3D problem. What is missing is a clear physical insulation between euchromatin and heterochromatin in three dimensions.

The solution to this problem might involve another player: heterochromatin protein 1 (HP1). This protein has the ability to form droplets in vitro and in vivo (through weak self-attraction) (135, 136) and has a specific binding site for the H3K9me3 tag (137–139). The ability of certain proteins to form biomolecular condensates through liquid–liquid phase separation has meanwhile become a major topic in biology (140). Chromosomes can be considered as block copolymers with blocks of H3K9me3-tagged nucleosomes and nucleosomes without the tag. Block copolymers localize at interfaces between two selective solvents (141); in the current system, H3K9me3 blocks form loops inside the HP1 droplets and the rest form loops outside the droplets. This geometry might recover after cell division even for the half-diluted H3K9me3 blocks. The H3K9 methylase Suv39h1, which has been found associated with HP1 (142, 143), can then put the missing tags back, with the HP1 droplets acting as a reaction container. Conditions in the nucleus might be such that HP1 droplets only form in the presence of methylated chromosome sections, a mechanism called polymer-assisted condensation (144), ensuring the right size and location of the condensates. Some elements of the above described scenario of epigenetic inheritance have been simulated

before (145), but other elements are missing, e.g., the rearrangement of chromosomes through cell division.

The scenario discussed so far concerns constitutive heterochromatin, which is always present in all cells. Chromatin packaging according to cell type might be achieved through facultative heterochromatin. Here, the tag is H3K27me3 and the role of HP1 might be played by polycomb repressive complex 1 (PCR1) (146). In addition, PCR1 is autocatalytic and puts a ubiquitin mark on histone H2A. H2A is known to be lost during DNA duplication (132) and even transcription (147). This might allow cells to sense which genes are needed in the cell and pack the chromosomes accordingly.

4. SUMMARY

This review article focusses on small- and large-scale structural and dynamic features of chromatin. The small scales are organized by the nucleosome, a highly dynamic DNA-protein complex that modulates the access of other DNA-binding proteins to the genetic material. I have emphasized the strong sensitivity of nucleosomal properties to the underlying base pair sequence. On large scales, nonconcatenated loops are an important theoretical concept to explain the overall structure of entire chromosomes. Surprisingly not just as a concept, true nonconcatenated loops play a crucial role in structuring interphase and mitotic chromosomes. Finally, I discussed how nucleosomes influence the large-scale structure of chromosomes through their epigenetic tags. The space allotted did not allow me to discuss other important subjects, such as correlated chromatin motion over several micrometers (148, 149) and the rheology of chromatin (150).

DISCLOSURE STATEMENT

The author is not aware of any affiliations, memberships, funding, or financial holdings that might be perceived as affecting the objectivity of this review.

ACKNOWLEDGMENTS

My own research on chromatin was done in collaboration with G.T. Barkema, R. Blossey, G. Brandani, RF. Bruinsma, J. Culkin, L. de Bruin, M. Emanuel, B. Eslami-Mossallam, R. Everaers, W.M. Gelbart, G. Lanzani, I.M. Kulić, H. Merlitz, F. Mohammad-Rafiee, L. Mollazadeh-Beidokhti, J. Neipel, R. Phillips, P. Prinsen, R.D. Schram, J.U. Sommer, M. Tompitak, C. Vaillant, K. van Deelen, J. van Noort, J. Widom, T. Yamamoto, M. Zuiddam, and many more. H.S. was supported by the Deutsche Forschungsgemeinschaft (DFG, German Research Foundation) under Germany's Excellence Strategy—EXC 2068—390729961—Cluster of Excellence Physics of Life of TU Dresden.

LITERATURE CITED

1. Schiessel H. 2003. *J. Phys. Condens. Matter* 15:R699–774
2. Luger K, Mäder AW, Richmond RK, Sargent DF, Richmond TJ. 1997. *Nature* 389:251–60
3. Ngo TTM, Zhang Q, Zhou R, Yodh JG, Ha T. 2015. *Cell* 160:1135–44
4. Eslami-Mossallam B, Schram RD, Tompitak M, van Noort J, Schiessel H. 2016. *PLOS ONE* 11:e0156905
5. Hall MA, Shundrovsky A, Bai L, Fulbright RM, Lis JT, Wang MD. 2009. *Nat. Struct. Mol. Biol.* 16:124–29
6. Bustamante C, Marko JF, Siggia ED, Smith S. 1994. *Science* 265:1599–600
7. Kaplan N, Moore IK, Fondufe-Mittendorf Y, Gossett AJ, Tillo D, et al. 2009. *Nature* 458:362–66
8. Lowary PT, Widom J. 1997. *PNAS* 94:1183–88
9. Satchwell SC, Drew HR, Travers AA. 1986. *J. Mol. Biol.* 191:659–75

10. Segal E, Fondufe-Mittendorf Y, Chen L, Thåström A, Field Y, et al. 2006. *Nature* 442:772–78
11. Jin H, Rube HT, Song JS. 2016. *Nucl. Acids Res.* 44:2047–57
12. Tillo D, Hughes TR. 2009. *BMC Bioinform.* 10:442
13. Locke G, Tolkunov D, Moqtaderi Z, Struhl K, Morozov AV. 2010. *PNAS* 107:20998–1003
14. Struhl K, Segal E. 2013. *Nat. Struct. Mol. Biol.* 20:267–73
15. Drillon G, Audit B, Argoul F, Arneodo A. 2016. *BMC Genom.* 17:526
16. Tompitak M, Vaillant C, Schiessel H. 2017. *Biophys. J.* 112:505–11
17. Olson WK, Gorin AA, Lu X-J, Hock LM, Zhurkin VB. 1998. *PNAS* 95:11163–68
18. Hinckley DM, Freeman GS, Whitmer JK, de Pablo JJ. 2013. *J. Phys. Chem.* 139:144903
19. Lankaš F, Šponer J, Langowski J, Cheatham TE III. 2003. *Biophys. J.* 85:2872–83
20. Morozov AV, Fortney K, Gaykalova DA, Studitsky VM, Widom J, Siggia ED. 2009. *Nucl. Acids Res.* 37:4707–22
21. Freeman GS, Lequieu JP, Hinckley DM, Whitmer JK, de Pablo JJ. 2014. *Phys. Rev. Lett.* 113:168101
22. Zuiddam M, Everaers R, Schiessel H. 2017. *Phys. Rev. E* 96:052412
23. Neipel J, Brandani G, Schiessel H. 2020. *Phys. Rev. E* 101:022405
24. Buenrostro JD, Giresi PG, Zaba LC, Chang HY, Greenleaf WJ. 2013. *Nat. Methods* 10:1213–18
25. Brogaard K, Xi L, Wang JP, Widom J. 2012. *Nature* 486:496–501
26. Kelly TK, Liu Y, Lay FD, Liang G, Berman BP, Jones PA. 2012. *Genome Res.* 22:2497–506
27. Kornberg RD, Stryer L. 1988. *Nucl. Acids Res.* 16:6677–90
28. Chevereau G, Palmeira L, Thermes C, Arneodo A, Vaillant C. 2009. *Phys. Rev. Lett.* 103:188103
29. Tillo D, Kaplan N, Moore IK, Fondufe-Mittendorf Y, Gossett AJ, et al. 2010. *PLOS ONE* 5:e9129
30. Vavouri T, Lehner B. 2011. *PLOS Genet.* 7:e1002036
31. Hammoud SS, Nix DA, Zhang H, Purwar J, Carrell DT, Cairns BR. 2009. *Nature* 460:473–78
32. Eslami-Mossallam B, Schiessel H, van Noort J. 2016. *Adv. Colloid Interface Sci.* 232:101–13
33. Fierz B, Poirier MG. 2019. *Annu. Rev. Biophys.* 48:321–45
34. Polach KJ, Widom J. 1995. *J. Mol. Biol.* 254:130–49
35. Anderson JD, Lowary PT, Widom J. 2001. *J. Mol. Biol.* 307:977–85
36. Li G, Widom J. 2004. *Nat. Struct. Mol. Biol.* 11:763–69
37. Li G, Levitus M, Bustamante C, Widom J. 2005. *Nat. Struct. Mol. Biol.* 12:46–53
38. Kelbauskas L, Chan N, Bash R, Yodh J, Woodbury N, Lohr D. 2007. *Biochemistry* 46:2239–48
39. Koopmans WJA, Brehm A, Logie C, Schmidt T, van Noort J. 2007. *J. Fluoresc.* 17:785–95
40. Moyle-Heyrman G, Tims HS, Widom J. 2011. *J. Mol. Biol.* 412:634–46
41. Tims HS, Gurunathan K, Levitus M, Widom J. 2011. *J. Mol. Biol.* 411:430–48
42. Gansen A, Felekyan S, Kühnemuth R, Lehmann K, Tóth K, et al. 2018. *Nat. Commun.* 9:4628
43. Konrad SF, Vanderlinden W, Frederickx W, Brouns T, Menze BH, et al. 2021. *Nanoscale* 13:5435–47
44. Konrad SF, Vanderlinden W, Lipfert J. 2022. *Biophys. J.* 121:841–51
45. Prinsen P, Schiessel H. 2010. *Biochimie* 92:1722–28
46. Anderson JD, Widom J. 2001. *Mol. Cell. Biol.* 21:3830–39
47. Kelbauskis L, Woodbury N, Lohr D. 2009. *Biochem. Cell Biol.* 87:323–35
48. Gansen A, Tóth, Schwarz N, Langowski J. 2009. *J. Phys. Chem. B* 113:2604–13
49. Tóth K, Böhm V, Sellmann C, Danner M, Hanne J, et al. 2013. *Cytometry A* 83:839–46
50. Lowary PT, Widom J. 1998. *J. Mol. Biol.* 276:19–42
51. Mauney AW, Tokuda JM, Gloss LM, Gonzalez O, Pollack M. 2018. *Biophys. J.* 115:773–81
52. van Deelen K, Schiessel H, de Bruin L. 2020. *Biophys. J.* 118:2297–308
53. Polach KJ, Widom J. 1996. *J. Mol. Biol.* 258:800–12
54. Culkin J, de Bruin L, Tompitak M, Phillips R, Schiessel H. 2017. *Eur. Phys. J. E* 40:106
55. Winogradoff D, Aksimentiev A. 2019. *J. Mol. Biol.* 431:323–35
56. Armeev GA, Kniazeva AS, Komarova GA, Kirpichnikov MP, Shaytan AK. 2021. *Nat. Commun.* 12:2387
57. Brower-Toland BD, Smith CL, Yeh RC, Lis JT, Peterson CL, Wang MD. 2002. *PNAS* 99:1960–65
58. Kulić IM, Schiessel H. 2004. *Phys. Rev. Lett.* 92:228101
59. Wocjan T, Klenin K, Langowski J. 2009. *J. Phys. Chem. B* 113:2639–46
60. Sudhanshu B, Mihardja S, Koslover EF, Mehraeen S, Bustamante C, Spakowitz AJ. 2011. *PNAS* 108:1885–90

61. Ettig R, Kepper N, Stehr R, Wedemann G, Rippe K. 2011. *Biophys. J.* 101:1999–2008
62. Mollazadeh-Beidokhti L, Mohammad-Rafiee F, Schiessel H. 2012. *Biophys. J.* 102:2235–40
63. Lanzani G, Schiessel H. 2012. *Europhys. Lett.* 100:48001
64. Mochrie SGJ, Mack AH, Schlingwein DJ, Collins R, Kamenetska M, Regan L. 2013. *Phys. Rev. E* 87:012710
65. Mack AH, Schlingman DJ, Salinas RD, Regan L, Mochrie SGJ. 2015. *J. Phys. Condens. Matter* 27:064106
66. Lequieu J, Córdoba A, Schwartz DC, de Pablo JJ. 2016. *ACS Cent. Sci.* 2:660–66
67. Khodabandeh F, Fatemi H, Mohammad-Rafiee F. 2020. *Soft Matter* 16:4806–13
68. Reddy G, Thirumalai D. 2021. *Nucl. Acids Res.* 49:4907–18
69. de Bruin L, Tompitak M, Eslami-Mossallam B, Schiessel H. 2016. *J. Phys. Chem. B* 120:5855–63
70. Tompitak M, de Bruin L, Eslami-Mossallam B, Schiessel H. 2017. *Phys. Rev. E* 95:052402
71. Durkin SG, Glover TW. 2007. *Annu. Rev. Genet.* 41:169–92
72. Chan KL, Palmai-Pallag T, Ying S, Hickson ID. 2009. *Nat. Cell Biol.* 11:753–60
73. Biebricher A, Hirano S, Enzlin JH, Wiechens N, Streicher WW, et al. 2013. *Mol. Cell* 51:691–701
74. Meersseman G, Pennings S, Bradbury EM. 1992. *EMBO J.* 11:2951–59
75. Kulić IM, Schiessel H. 2003. *Phys. Rev. Lett.* 91:148103
76. Mohammad-Rafiee F, Kulić IM, Schiessel H. 2004. *J. Mol. Biol.* 344:47–58
77. Brandani GB, Niina T, Tan C, Takada S. 2018. *Nucl. Acids Res.* 46:2788–801
78. Schiessel H, Widom J, Bruinsma RF, Gelbart WM. 2001. *Phys. Rev. Lett.* 86:4414–17
79. Kulić IM, Schiessel H. 2003. *Biophys. J.* 84:3197–211
80. Lequieu J, Schwartz DC, de Pablo JJ. 2017. *PNAS* 114:E9197–205
81. Niina T, Brandani GB, Tan C, Takada S. 2017. *PLOS Comput. Biol.* 13:e1005880
82. Rudnizky S, Khamis H, Malik O, Melamed P, Kaplan A. 2019. *PNAS* 116:12161–66
83. Winger J, Nodelman IM, Levendosky RF, Bowman GD. 2018. *eLife* 7:e34100
84. Li M, Xia X, Tian Y, Jia Q, Liu X, et al. 2019. *Nature* 567:409–13
85. Sabantsev A, Levendosky RF, Zhuang X, Bowman GD, Deindl S. 2019. *Nat. Commun.* 10:1720
86. Brandani GB, Takada S. 2018. *PLOS Comput. Biol.* 14:e1006512
87. Segal E, Widom J. 2009. *Trend Genet.* 25:335–43
88. Nodelman IM, Das S, Faustino AM, Fried SD, Bowman GD, Armache JP. 2022. *Nat. Struct. Mol. Biol.* 29:121–29
89. Narlikar GJ. 2010. *Curr. Opin. Chem. Biol.* 14:660–65
90. Schiessel H, Blossey R. 2020. *Phys. Rev. E* 101:040401(R)
91. Eltsov M, MacLellan KM, Maeshima K, Frangakis AS, Dubochet J. 2008. *PNAS* 105:19732–37
92. Joti Y, Hikima T, Nishino Y, Kamada F, Hihara S, et al. 2012. *Nucleus* 3:404–10
93. Ricci MA, Manzo C, García-Parajo MF, Lakadamyali M, Cosma MP. 2015. *Cell* 160:1145–58
94. Portillo-Ledesma S, Tsao LH, Wagley M, Lakadamyali M, Cosma MP, Schlick T. 2021. *J. Mol. Biol.* 433:166701
95. Sazer S, Schiessel H. 2018. *Traffic* 19:87–104
96. de Gennes PG. 1979. *Scaling Concepts in Polymer Physics*. Ithaka, NY: Cornell Univ. Press
97. van den Engh G, Sachs R, Trask BJ. 1992. *Science* 257:1410–12
98. Bolzer A, Kreth G, Solovei I, Koehler D, Saracoglu K, et al. 2005. *PLOS Biol.* 3:e157
99. Emanuel M, Radja NH, Henriksson A, Schiessel H. 2009. *Phys. Biol.* 6:025008
100. Mateos-Langerak J, Bohn M, de Leeuw W, Giromus O, Manders EMM, et al. 2009. *PNAS* 106:3812–17
101. Maeshima K, Rogge R, Tamura S, Joti Y, Hikima T, et al. 2016. *EMBO J.* 35:1115–32
102. Gibson BA, Doolittle LK, Schneider MWG, Jensen LE, Gamarra N, et al. 2019. *Cell* 179:470–84
103. Strickfaden H, Tolsma TO, Sharma A, Underhill DA, Hansen JC, Hendzel MJ. 2020. *Cell* 183:1772–84
104. Bajpai G, Pavlov DA, Lorber D, Volk T, Safran S. 2021. *eLife* 10:e63976
105. Amiad-Pavlov D, Lorber D, Bajpai G, Reuveny A, Roncato F, et al. 2021. *Sci. Adv.* 7:eabf6251
106. Farr SE, Woods EJ, Joseph JA, Garaizar A, Collepardo-Guevara R. 2021. *Nat. Commun.* 12:2883
107. Lua R, Borovinskiy AL, Grosberg AY. 2004. *Polymer* 45:717–31
108. Lieberman-Aiden E, van Berkum NL, Williams L, Imakaev M, Ragoczy T, et al. 2009. *Science* 326:289–93

109. Grosberg A, Rabin R, Havlin S, Neer A. 1993. *Europhys. Lett.* 23:373–78
110. Smrek J, Grosberg AY. 2013. *Physica A* 392:6375–88
111. Schram RD, Barkema GT, Schiessel H. 2013. *J. Chem. Phys.* 138:224901
112. Sikorav JL, Jannink G. 1994. *Biophys. J.* 66:827–37
113. Rosa A, Everaers R. 2008. *PLOS Comput. Biol.* 4:e1000153
114. Schiessel H. 2022. *Biophysics for Beginners: A Journey Through the Cell Nucleus*. Singapore: Jenny Stanford Publ. 2nd ed.
115. Halverson JD, Lee WB, Grest GS, Grosberg AY, Kremer K. 2011. *J. Chem. Phys.* 134:204904
116. Rosa A, Everaers R. 2014. *Phys. Rev. Lett.* 112:118302
117. Rao SSP, Huntley MH, Durand NC, Stamenova EK, Bochkov ID, et al. 2014. *Cell* 159:1665–80
118. Golfier S, Quail T, Kimura H, Brugués. 2020. *eLife* 9:e53885
119. Fudenberg G, Imakaev M, Lu C, Goloborodko A, Mirny LA. 2016. *Cell Rep.* 15:2038–49
120. Banigan EJ, van den Berg AA, Brandão HB, Marko JF, Mirny LA. 2020. *eLife* 9:e53558
121. Banigan EJ, Mirny LA. 2020. *eLife* 9:e63528
122. Sanborn AL, Rao SSP, Huang SC, Durand NC, Huntley MH, et al. 2015. *PNAS* 112:E6456–65
123. Grosberg AY, Khalatur PG, Khokhlov AR. 1982. *Makromol. Chem. Rapid Commun.* 3:709–13
124. Terakawa T, Bisht S, Eeftens JM, Dekker C, Haering CH, Greene EC. 2017. *Science* 358:672–76
125. Ganji M, Shaltiel IA, Bisht S, Kim E, Kalichava A, et al. 2018. *Science* 360:102–5
126. Gibcus JH, Samejima K, Goloborodko A, Samejima I, Naumova N, et al. 2018. *Science* 359:eaao6135
127. Goloborodko A, Imakaev MV, Marko JF, Mirny L. 2016. *eLife* 5:e14864
128. Shintomi K, Inoue F, Watanabe H, Ohsumi K, Ohsugi M, Hirano T. 2017. *Science* 356:1284–87
129. Shintomi K, Hirano T. 2021. *Nat. Commun.* 12:2917
130. Yamamoto T, Schiessel H. 2022. *Biophys. J.* 121(14):2742–50
131. Cortini R, Barbi M, Caré BR, Lavelle C, Lesne A, et al. 2016. *Rev. Mod. Phys.* 88:025002
132. Yu C, Gan H, Serra-Cardona A, Zhang L, Gan S, et al. 2018. *Science* 361:1386–89
133. Barkess G, West AG. 2012. *Epigenomics* 4:67–80
134. Gazner M, Felsenfeld G. 2006. *Nat. Rev.* 7:703–13
135. Larson AG, Elnatan D, Keenen MM, Trnka MJ, Johnston JB, et al. 2017. *Nature* 547:236–40
136. Strom AR, Emelyanov AV, Mir M, Fyodorov DV, Darzacq X, Karpen GH. 2017. *Nature* 547:241–45
137. Bannister AJ, Zegerman P, Partridge JF, Miska EA, Thomas JO, et al. 2001. *Nature* 410:120–24
138. Lachner M, O'Carroll D, Rea S, Mechtler K, Jenuwein T. 2001. *Nature* 410:116–20
139. Nakayama J, Rice JC, Strahl BD, Allis CD, Grewal SIS. 2001. *Science* 292:110–13
140. Banani SF, Lee HO, Hyman AA, Rosen MK. 2017. *Nat. Rev. Mol. Cell Biol.* 18:285–98
141. Sommer J-U, Daoud M. 1996. *Phys. Rev. E* 53:905–20
142. Aagaard L, Laible G, Selenko P, Schmid M, Dorn R, et al. 1999. *EMBO J.* 18:1923–38
143. Raurell-Vila H, Bosch-Presegue L, Gonzalez J, Kane-Goldsmith N, Casal C, et al. 2017. *Epigenetics* 12:166–75
144. Sommer J-U, Merlitz H, Schiessel H. 2022. *Macromolecules* 55(11):4841–51
145. Sandholtz SH, MacPherson Q, Spakowitz AJ. 2020. *PNAS* 117:20423–29
146. Eeftens JM, Kapoor M, Michieletto D, Brangwynne CP. 2021. *Nat. Commun.* 12:5888
147. Kireeva ML, Walter W, Tchernajenko V, Bondarenko V, Kashlev M, Studitsky VM. 2002. *Mol. Cell* 9:541–52
148. Zidovska A, Weitz DA, Mitchison TJ. 2013. *PNAS* 110:15555–60
149. Shaban HA, Barth R, Bystricky K. 2018. *Nucl. Acids Res.* 46:e77
150. Eshghi I, Eaton JA, Zidovska A. 2021. *Phys. Rev. Lett.* 126:228101

Annual Review of Condensed Matter Physics

Volume 14, 2023

Contents

Errata

An online log of corrections to *Annual Review of Condensed Matter Physics* articles may be found at http://www.annualreviews.org/errata/conmatphys